

Testing the theory of QGP-induced energy loss at RHIC and the LHC

Ivan Vitev

*Los Alamos National Laboratory, Theoretical Division and Physics Division,
Mail Stop H846, Los Alamos, NM 87545, USA*

(Dated: July 5, 2018)

We compare an analytic model of jet quenching, based on the GLV non-Abelian energy loss formalism, to numerical results for the centrality dependent suppression of hadron cross sections in Au+Au and Cu+Cu collisions at RHIC. Simulations of neutral pion quenching versus the size of the colliding nuclear system are presented to high transverse momentum p_T . At low and moderate p_T , we study the contribution of medium-induced gluon bremsstrahlung to single inclusive hadron production. In Pb+Pb collisions at the LHC, the redistribution of the lost energy is shown to play a critical role in yielding nuclear suppression that does not violate the participant scaling limit.

PACS numbers: 12.38.Bx, 12.38.Mh, 25.75.-q

I. INTRODUCTION

Strong suppression of single inclusive pions and charged hadrons at large transverse momentum, as large as $p_T = 20$ GeV [1, 2], is arguably one of the most fascinating phenomena from the heavy ion program at the Relativistic Heavy Ion Collider (RHIC). It signifies the transition from soft, collective and strongly model-dependent physics to the high p_T or E_T production of particles and jets that is well understood in terms of the perturbative Quantum Chromodynamics (pQCD) factorization approach. Calibrated hard probes can thus be used to sample the properties of the medium created in collisions of heavy nuclei [3]. With capabilities to detect $p_T \sim 50$ GeV pions and $E_T \sim 500$ GeV jets with good statistics, experiments at the Large Hadron Collider (LHC) will be able to critically test such perturbative calculations of hadron and jet modification in the quark-gluon plasma (QGP) at a new energy frontier.

Following the discovery [4] of jet quenching in Au+Au collisions and its verification through d+Au measurements [5] at RHIC, heavy ion theory has emphasized the need for a systematic study of the energy and system size dependence of leading particle attenuation [3, 6]. Previous measurements have been limited to transverse momenta $p_T \leq 10$ GeV and Au+Au collisions at RHIC [7]. More recent results up to $p_T \sim 20$ GeV [1, 2] in both Au+Au and Cu+Cu reactions were shown to be compatible with several theoretical estimates, emphasizing the final state QGP-induced suppression of jets [6, 8, 9]. In this Letter, we compare for the first time analytic [3] and numerical [6] models of jet absorption in order to establish the role of sub-leading effects, such as the running of the strong coupling constant α_s with the Debye screening scale $\mu \simeq gT$ in the plasma. We present our predictions for π^0 quenching versus centrality, p_T and \sqrt{s} , based on the Gyulassy-Levai-Vitev (GLV) approach to the medium-induced non-Abelian energy loss [10]. We note that redistribution of the lost energy in small and moderate p_T hadrons plays a significant role in the transition from high p_T suppression to low p_T enhancement of the back-to-back two particle correlations [11]. In this

Letter we give results for single inclusive pions and identify the range of transverse momenta at RHIC and the LHC where the gluon feedback is important.

In Section II we present a simple analytic model for the system size, N_{part} , dependence of jet quenching in nucleus-nucleus collisions. Section III contains select intermediate results from the GLV theory, including the evaluation of the mean gluon number $\langle N_g \rangle$ and fractional energy loss $\langle \Delta E/E \rangle$. The derivation of the radiative gluon contribution to small and moderate p_T hadron production is given in Section IV. Section V presents the calculated suppression of π^0 production in Cu+Cu and Au+Au collisions at RHIC and Pb+Pb collisions at the LHC. Conclusions are given in Section VI.

II. ANALYTIC MODEL OF JET QUENCHING

While tomographic determination of the properties of the medium created in nucleus-nucleus collisions can only be achieved through detailed numerical simulations, it is useful to define a simplified analytic model which incorporates the essential features of jet quenching calculations. We first review the approach formulated in [3] and discuss its advantages and limitations.

The final state medium-induced energy loss occurs after the hard partonic scattering $ab \rightarrow cd$ and before the fragmentation of the parent parton into a jet of colorless hadrons. We consider for simplicity high $p_T > 5$ GeV hadron production at RHIC and will show later that the contribution of the induced bremsstrahlung in this region is small. There are two equivalent ways of implementing energy loss in the perturbative QCD hadron production formalism. The first one associates ΔE with the kinematic modification of the momentum fraction $z = p_h^+/p_c^+$ in the fragmentation function $D_{h/c}(z)$, leaving the hard parton production cross section $d\sigma^c/dy d^2p_{Tc}$ unmodified. The second approach reduces the jet cross section in the presence of the medium but leaves $D_{h/c}(z)$ unaltered. It can conveniently be implemented in an analytic model of QGP-induced leading hadron suppression. We take the underlying parton production cross section to be of

power law type

$$\frac{d\sigma^c}{dyd^2p_{T_c}} = \frac{A}{(p_0 + p_{T_c})^n} \approx \frac{A}{p_{T_c}^n}, \quad \text{if } p_{T_c} \gg p_0, \quad (1)$$

where $n = n(y, p_{T_c}, \sqrt{s})$ and $p_0 \sim 2.5$ GeV at RHIC. In a finite p_T range, fixed rapidity y and center of mass energy \sqrt{s} , a constant $n = \langle n(y, p_{T_c}, \sqrt{s}) \rangle$ is a good approximation. At RHIC, in the region of $5 \text{ GeV} < p_{T_c} < 10 \text{ GeV}$, the spectra scale roughly as $n_q = 7$, $n_g = 8.4$. Fragmentation functions are convoluted with the partonic cross section as follows

$$\begin{aligned} \frac{d\sigma^h}{dyd^2p_T} &= \sum_c \int_{z_{\min}}^1 dz \frac{d\sigma^c(p_c = p_T/z)}{dyd^2p_{T_c}} \frac{1}{z^2} D_{h/c}(z) \\ &\approx \sum_c \frac{d\sigma^c(p_T/\langle z \rangle)}{dyd^2p_{T_c}} \frac{1}{\langle z \rangle^2} D_{h/c}(\langle z \rangle) \\ &\approx \sum_c \frac{A}{p_{T_c}^n} \langle z \rangle^{(n-2)} D_{h/c}(\langle z \rangle) \end{aligned} \quad (2)$$

In Eq. (2) $z_{\min} = p_T/p_{T_c \text{ max}}$ and the subsequent approximation is most reliable when $z_{\min} \ll 1$. It should be noted that $\langle z \rangle$ will also depend on the partonic and hadronic species.

The second input to the analytic model comes from the radiative energy loss formalism [10]. To understand the system size dependence of jet quenching, we use the approximate GLV formula which relates ΔE to the size and the soft parton rapidity density of the medium. For (1+1)D Bjorken expansion, in the limit of large parton energy $2E/\mu^2L \gg 1$, we find [12]

$$\frac{\Delta E}{E} \approx \frac{9C_R\pi\alpha_s^3}{4} \frac{1}{A_\perp} \frac{dN^g}{dy} L \frac{1}{E} \ln \frac{2E}{\mu^2L} + \dots \quad (3)$$

In Eq. (3) L is the jet path length in the medium and A_\perp is the transverse area. $C_R = 4/3$ (3) for quarks (gluons), respectively, is the quadratic Casimir in the fundamental (adjoint) representation of SU(3). Numerical simulations of $\Delta E/E$ clearly indicate a weaker dependence of the fractional energy loss on the jet energy than given in Eq. (3).

The key to understanding the dependence of jet quenching on the heavy ion species and centrality is the effective atomic mass number, A_{eff} , or the number of participants, N_{part} , dependence of the characteristic plasma parameters in Eq. (3) [3],

$$dN^g/dy \propto dN^h/dy \propto A_{\text{eff}} \propto N_{\text{part}}, \quad (4)$$

$$L \propto A_{\text{eff}}^{1/3} \propto N_{\text{part}}^{1/3}, \quad A_\perp \propto A_{\text{eff}}^{2/3} \propto N_{\text{part}}^{2/3}. \quad (5)$$

Therefore, the *fractional* energy loss scales approximately as

$$\epsilon = \Delta E/E \propto A_{\text{eff}}^{2/3} \propto N_{\text{part}}^{2/3}, \quad (6)$$

up to logarithmic corrections from Eq. (3). If a parton loses this momentum fraction ϵ during its propagation in

the medium to escape with momentum $p_{T_c}^{\text{quench}}$, immediately after the hard collision $p_{T_c} = p_{T_c}^{\text{quench}}/(1 - \epsilon)$. Noting the additional Jacobian $|d^2p_{T_c}^{\text{quench}}/d^2p_{T_c}| = (1 - \epsilon)^2$, we find for the quenched hadronic spectrum per elementary NN collision

$$\begin{aligned} \frac{d\sigma_{\text{quench}}^h}{dyd^2p_T} &= \sum_c \frac{d\sigma^c(p_T/(1 - \epsilon)\langle z \rangle)}{dyd^2p_{T_c}} \frac{1}{(1 - \epsilon)^2 \langle z \rangle^2} D_{h/c}(\langle z \rangle) \\ &\approx (1 - \epsilon_{\text{eff}})^{n-2} \sum_c \frac{A}{p_{T_c}^n} \langle z \rangle^{(n-2)} D_{h/c}(\langle z \rangle). \end{aligned} \quad (7)$$

In Eq. (7) ϵ_{eff} is the average over all parton species and accounts for the color charge, geometry and multi-gluon fluctuations. From this result we can easily derive the system size dependence of the nuclear modification factor

$$\begin{aligned} R_{AA} &= \frac{\sigma_{pp}^{\text{in}}}{N_{AA \text{ col}}} \frac{dN_{AA}^h/dyd^2p_T}{d\sigma^h/dyd^2p_T} \quad (\text{exp.}) \\ &\approx \frac{d\sigma_{\text{quench}}^h/dyd^2p_T}{d\sigma^h/dyd^2p_T} \quad (\text{th.}) \\ &= (1 - \epsilon_{\text{eff}})^{n-2} = \left(1 - \frac{k}{n-2} N_{\text{part}}^{2/3}\right)^{n-2}. \end{aligned} \quad (8)$$

In Eq. (8) $k/(n-2)$ is the proportionality coefficient in Eq. (6) which depends on the microscopic properties of the medium but not on its size. With $n \gg 1$ and experimentally measured and theoretically calculated suppression, ~ 5 fold in central Au+Au collisions at RHIC, $\epsilon_{\text{eff}} = N_{\text{part}}^{2/3} k/(n-2)$ is small. We thus predict that the *logarithm* of nuclear suppression, Eq. (8), has simple power law dependence on the system size

$$\ln R_{AA} = -k N_{\text{part}}^{2/3}, \quad (9)$$

where the leading correction goes as $k^2 N_{\text{part}}^{4/3}/2(n-2)$.

We focus on the most central nuclear collisions and use impact parameters $b = 1 - 3$ fm depending on the atomic mass A . An optical Glauber model calculation is used to evaluate $N_{\text{part}}^{2/3}$ with $\sigma_{pp}^{\text{in}} = 42$ mb and a Wood-Saxon nuclear density with results given in Table I. The analytic prediction for the system size dependence of jet quenching is shown in Fig. 1. It is fixed by the magnitude of the suppression established in central Au+Au collisions [7] and consistent with existing simulations [12]. From this analysis we expect a factor ~ 2 suppression in

Species	⁹ Be	¹⁶ O	²⁸ Si	³² S	⁵⁶ Fe	⁶⁴ Cu	¹⁹⁷ Au	²⁰⁸ Pb	²³⁸ U
b [fm]	1	1	1.5	1.5	2	2	3	3	3
$N_{\text{part}}^{2/3}$	5	8	12	14	20	22	48	50	55

TABLE I: Summary of the relevant quenching parameter $N_{\text{part}}^{2/3}$ (rounded) at a fixed impact parameter b for select heavy ion species.

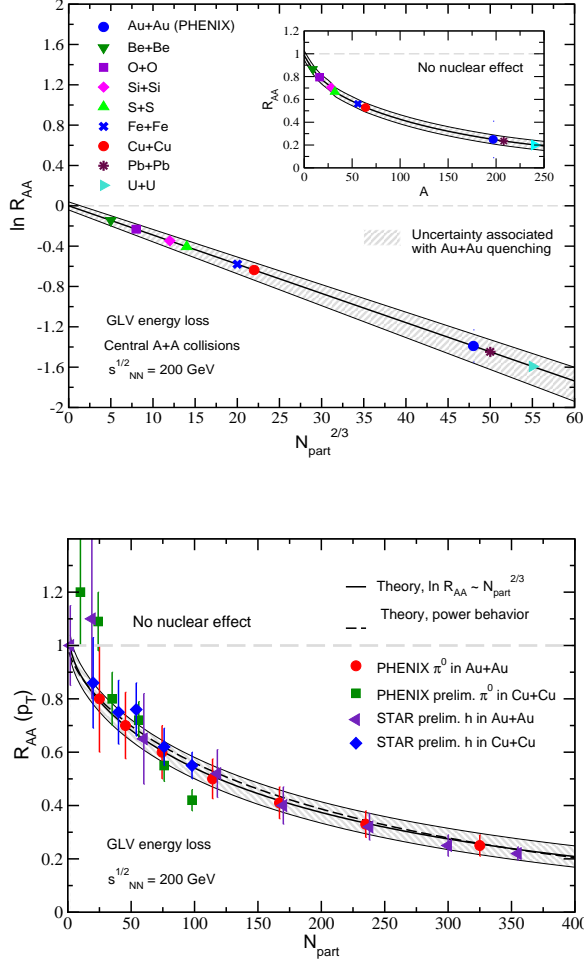


FIG. 1: Top panel: the predicted linear dependence of jet quenching in natural variables, $\ln R_{AA}$ versus $N_{part}^{2/3}$, for central collisions of ${}^9\text{Be}$, ${}^{16}\text{O}$, ${}^{28}\text{Si}$, ${}^{32}\text{S}$, ${}^{56}\text{Fe}$, ${}^{64}\text{Cu}$, ${}^{208}\text{Pb}$ and ${}^{238}\text{U}$. Bottom panel: comparison of the analytic R_{AA} to PHENIX and STAR experimental data in Au+Au and Cu+Cu collisions.

central Cu+Cu collisions. Comparison to the preliminary PHENIX $p_T > 7$ GeV data [1] and STAR $p_T > 6$ GeV data [2] is also shown in the bottom panel of Fig. 1 with good agreement within the experimental uncertainties. Dashed and solid lines illustrate the difference between Eqs. (8) and (9) when normalized to the same suppression in central Au+Au collisions.

The main advantage of the GLV analytic model is the ability to provide guidance on the magnitude of the QGP-induced jet quenching versus centrality and address a large body of experimental data. Its limitations include a fixed coupling constant α_s , implementation of only the mean, though suitably reduced, energy loss ΔE and the inability to incorporate additional nuclear effects, such as the Cronin multiple scattering [5] and nuclear shadowing [14]. It also relies on a reference numerical calculation in central A+A collisions in the same p_T and y range as well as \sqrt{s} [12]. The deviation of dN^g/dy from the exact

participant scaling in Eq. (4) may lead to less quenching and improved agreement with the data in peripheral reactions, but is here neglected.

III. NUMERICAL EVALUATION OF THE QGP-INDUCED ENERGY LOSS

The solution for the differential in energy (ω) and transverse momentum (\mathbf{k}) spectrum of medium induced gluon radiation has been obtained order by order in the correlations between the multiple scattering centers in nuclear matter using the reaction operator approach [10]

$$\begin{aligned} \omega \frac{dN_g}{d\omega d^2\mathbf{k}} &\approx \sum_{n=1}^{\infty} \frac{C_R \alpha_s}{\pi^2} \prod_{i=1}^n \int_0^{L - \sum_{a=1}^{i-1} \Delta z_a} \frac{d\Delta z_i}{\lambda_g(i)} \\ &\times \int d^2\mathbf{q}_i \left[\sigma_{el}^{-1}(i) \frac{d\sigma_{el}(i)}{d^2\mathbf{q}_i} - \delta^2(\mathbf{q}_i) \right] \\ &\times \left(-2 \mathbf{C}_{(1, \dots, n)} \cdot \sum_{m=1}^n \mathbf{B}_{(m+1, \dots, n)(m, \dots, n)} \right. \\ &\times \left[\cos \left(\sum_{k=2}^m \omega_{(k, \dots, n)} \Delta z_k \right) \right. \\ &\left. \left. - \cos \left(\sum_{k=1}^m \omega_{(k, \dots, n)} \Delta z_k \right) \right] \right). \quad (10) \end{aligned}$$

Here \mathbf{q}_i are the momentum transfers from the medium, distributed according to a normalized elastic differential cross section $\sigma_{el}(i)^{-1} d\sigma_{el}(i)/d^2\mathbf{q}_i$, and $\Delta z_k = z_k - z_{k-1}$ are the separations of the subsequent scattering centers. In Eq. (10) the color current propagators and inverse formation times are denoted by

$$\begin{aligned} \mathbf{C}_{(m, \dots, n)} &= \frac{1}{2} \nabla_{\mathbf{k}} \ln (\mathbf{k} - \mathbf{q}_m - \dots - \mathbf{q}_n)^2, \\ \mathbf{B}_{(m+1, \dots, n)(m, \dots, n)} &= \mathbf{C}_{(m+1, \dots, n)} - \mathbf{C}_{(m, \dots, n)}, \\ \omega_{(m, \dots, n)} &= \frac{(\mathbf{k} - \mathbf{q}_m - \dots - \mathbf{q}_n)^2}{2\omega}. \quad (11) \end{aligned}$$

Numerical results have been obtained to third order in the opacity, $\langle L/\lambda_g \rangle$, with all correlations of up to four scattering centers, including the initial hard interaction. To speed up the evaluation of the squared amplitudes, the oscillating quantum coherence phases between the points of interaction were converted to Lorentzians using an exponentially falling geometry with no sharp edges. The requirement that the mean locations z_k , $k = 1 \dots n$ of n scatterers are the same as the one for a uniform soft parton distribution fixes the parameter L_e of such geometry [10]:

$$\langle z_0 - z_k \rangle = k \frac{L}{n+1} \quad \rightarrow \quad L_e = \frac{L}{n+1}. \quad (12)$$

Bjorken (1+1)D expansion of the plasma is accounted for as follows:

$$\rho(z_k) = \rho(z_0) \frac{z_0}{z_k},$$

$$\mu(z_k) = \mu(z_0) \left(\frac{z_0}{z_k} \right)^{1/3}, \quad \lambda_g(z_k) = \lambda_g(z_0) \left(\frac{z_k}{z_0} \right)^{1/3}, \quad (13)$$

and the kinematic constraints,

$$\mu/Q \leq x = k^+/E^+ \approx \omega/E \leq 1,$$

$$\mu \leq |\mathbf{k}| \leq \sqrt{Q^2} \min(x, 1-x), \quad (14)$$

have been incorporated for consistency with our previous work [12]. It was recently shown that for physical on-shell final state gluons the medium induced radiation is infrared and collinear safe [11]. This allows relaxation of the $\mu/Q \leq x$, $\mu \leq |\mathbf{k}|$ constraints in the future, though it should be noted that the Debye screening scale still controls the small \mathbf{k} and ω cancellation between the single and double Born diagrams in the opacity expansion [10].

To evaluate the effect of multiple gluon emission and arrive at a probabilistic distribution $P(\epsilon)$ for the fractional energy loss $\epsilon = \Delta E/E = \sum_{i=1}^n \epsilon_i$, $\epsilon_i = \omega_i/E$, we are motivated by an independent Poisson gluon emission ansatz, but incorporate kinematic constraints [13]:

$$P(\epsilon) = \sum_{n=0}^{\infty} P_n(\epsilon), \quad P_0(\epsilon) = e^{-\langle N_g \rangle} \delta(\epsilon),$$

$$P_n(\epsilon) = \frac{1}{n} \int_0^{\epsilon} d\epsilon' P_{n-1}(\epsilon - \epsilon') \frac{dN_g}{d\epsilon'}(\epsilon' = \omega/E). \quad (15)$$

We normalize this probability density to unity and Eq. (15) ensures that at every step energy is conserved. As a consequence, for small jet energies and large $\Delta E/E$ the gluon distribution is distinctly non-Poisson. We evaluate the mean energy loss as follows:

$$\int_0^1 d\epsilon P(\epsilon) = 1, \quad \int_0^1 d\epsilon \epsilon P(\epsilon) = \left\langle \frac{\Delta E}{E} \right\rangle. \quad (16)$$

In Ref. [12] we considered jet production following the binary collision density $T_{AA}(b)$ in central Au+Au reactions at $\sqrt{s} = 200$ GeV. In an elementary hard interaction inclusive jets are distributed uniformly in azimuth relative to the reaction plane. We calculated $\langle \langle \Delta E \rangle \rangle_{\text{geom.}}$ using the line integral, Eq. (10), through the (1+1)D Bjorken expanding medium density by correctly weighing the amount of lost energy with the jet production rate. Cylindrical geometry with radius $L = 6$ fm that gives the same mean energy loss $\langle \Delta E \rangle$ for uniform initial soft parton rapidity density was then constrained. Using Eqs. (4) and (5) we can determine the effective length L , transverse area $A_{\perp} = \pi L^2$, gluon rapidity density dN_g/dy and effective atomic mass A_{eff} for shadowing applications [14] in interacting heavy ion systems of different size. Table II summarizes the parameters used in our calculation of central, mid-central

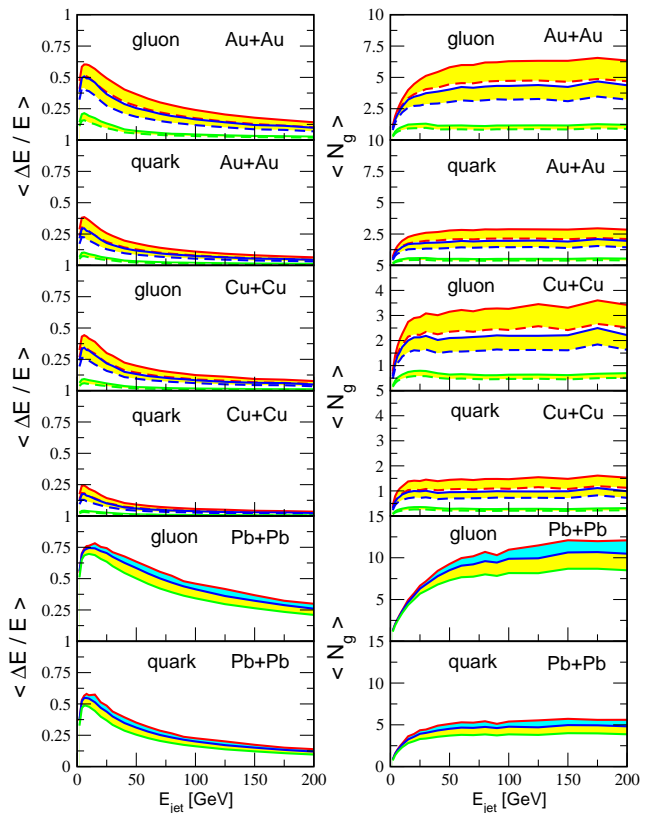


FIG. 2: Left panel: mean energy loss for Au+Au and Cu+Cu soft parton densities at RHIC corresponding to centralities given in Table II and Pb+Pb soft parton densities at the LHC corresponding to central collisions versus the jet energy. Right panel: mean gluon number versus E_{jet} for the same heavy ion systems.

and peripheral Au+Au and Cu+Cu collisions at $\sqrt{s} = 200$ GeV at RHIC. For central collisions with $\sqrt{s} = 5.5$ TeV at the LHC, we use $dN_g/dy = 2000, 3000$ and 4000 to test the sensitivity of jet quenching to the QGP

Centrality	0 – 10%	20 – 30%	60 – 80%
N_{part}	328	167	21
dN_g/dy	800 - 1175	410 - 600	50 - 75
L [fm]	6	4.8	2.4
A_{eff}	197	99	12

Centrality	0 – 10%	20 – 30%	60 – 80%
N_{part}	103	55	9
dN_g/dy	255 - 370	135 - 195	20 - 30
L [fm]	4.1	3.3	1.8
A_{eff}	64	34	6

TABLE II: Estimated dN_g/dy , L and A_{eff} versus N_{part} for central, semi-central and peripheral Au+Au (top table) and Cu+Cu (bottom table) at RHIC.

properties.

The calculated fractional energy loss and mean gluon number for quark and gluon jets versus their energy for the centralities and densities discussed above are shown in the left and right panels of Fig. 2. Only in the limit $E_{jet} \rightarrow \infty$, $\Delta E/E \rightarrow 0$ does the energy loss for quarks and gluons approach the naive ratio $\Delta E^g/\Delta E^q = C_A/C_F = 9/4$. For large fractional energy losses this ratio is determined by the $\Delta E \leq E$ constraint. In this regime no simple scaling arguments related to the properties of the dense nuclear matter and the color charge are applicable. It should be noted that at high E_{jet} the fractional energy loss is not large even at the LHC.

In our calculation the strong coupling constant α_s is not used as a free parameter but evaluated at the typical scale μ in the elastic scattering cross section $\sigma_{el}(i)$ and the gluon mean free path $\lambda_g(i) = 1/\sigma_{el}(i)\rho(i)$. At the radiation vertex, $\alpha_s(\mathbf{k}^2)$ is also sensitive to the increase of the temperature or density of the medium, $\rho \propto T^3$, with the increase of dN^g/dy at a fixed transverse area A_\perp . The effects described here lead to sub-linear dependence of the energy loss on dN^g/dy . For the LHC example, given in Fig. 2, this can be a 50% correction for large E_{jet} and even more significant at low E_{jet} when compared to Eq. (3). Conversely, at low parton densities in peripheral collisions the energy loss will be larger than naively expected.

Another important point, seen in the right panel of Fig. 2, is that except for very low jet energies the mean gluon number $\langle N_g \rangle$ is not small ($\ll 1$) and the probability of not radiating gluons, $P_0 = \exp(-\langle N_g \rangle)$, is never large. Full results for $P(\epsilon)$ were shown in [8, 13]. We find that the probability density *does not* approximate $a\delta(\epsilon) + (1-a)\delta(1-\epsilon)$, $a < 1$. The latter ansatz yields $R_{AA}(p_T) = a$ independent on the collision energy or p_T . Instead, $P(\epsilon)$ is much more uniformly distributed in the interval $[0, 1]$ and our calculations retain sensitivity to the local slope and the parton species contribution to the differential inclusive hadron production cross section, see Eq. (8).

We finally note that multi-gluon fluctuations, given by Eq. (15), reduce the jet quenching effect relative to the application of the mean $\langle \Delta E/E \rangle$ shown in Fig. 2 [13]. This can be seen by comparing the $\epsilon_{\text{eff}} \approx 0.2$ in central Au+Au reactions, obtained from Eq. (8), to the fractional energy loss for 10 GeV quark jets, $\epsilon_{\text{eff}} < \langle \Delta E/E \rangle$. To investigate the scaling of energy loss with N_{part} we select quark jets of $E_{jet} = 10, 20$ and 30 GeV at midrapidity at RHIC and $N_{\text{part}} = 9, 21, 55, 103, 167$ and 328. These cover fractional energy losses $0 < \langle \Delta E/E \rangle < 0.4$ with numerical results shown in Fig. 3. Power law fits, also plotted, give exponents $n = 0.60 - 0.63$ that are not very different from the naive $n = 2/3$ expectation from Eq. (6) that was used in Fig. 1. We conclude that the deviation between the calculated energy loss with kinematic constraints and running strong coupling constants and its asymptotic fixed α_s analytic behavior is smaller when the variation of the energy loss is associated with a change in the system size rather than a large change in

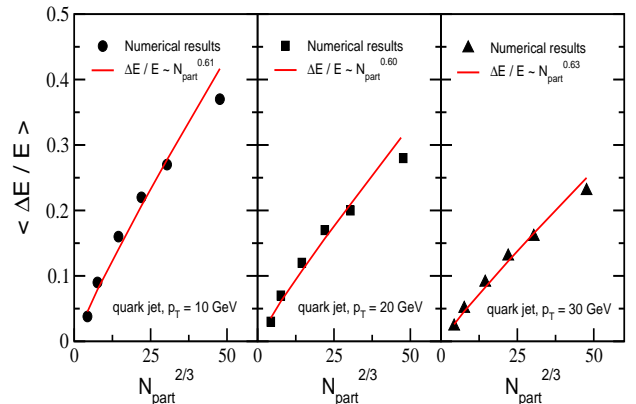


FIG. 3: N_{part} dependence of the fractional energy loss $\Delta E/E$ for $E_{jet} = 10, 20$ and 30 GeV quark jets in $\sqrt{s} = 200$ GeV nucleus-nucleus collisions. Power law fits yield exponents $n = 0.61, 0.60$ and 0.63, respectively.

the density of the medium alone.

IV. NUCLEAR EFFECTS ON INCLUSIVE HADRON PRODUCTION

The lowest order perturbative QCD cross section for single inclusive hadrons in nucleon-nucleon (NN) reactions, including non-vanishing transverse momentum $\mathbf{k}_{a,b}$ distributions of the incoming partons, is given by

$$\begin{aligned} \frac{d\sigma_{NN}^h}{dyd^2p_T} &= K \sum_{abcd} \int_{x_{a \min}}^1 \int_{x_{b \min}}^1 dx_a dx_b \int d^2\mathbf{k}_a d^2\mathbf{k}_b \\ &\times f(\mathbf{k}_a) f(\mathbf{k}_b) \phi_{a/N}(x_a, \mu_f) \phi_{b/N}(x_b, \mu_f) \\ &\times \frac{1}{\pi z_c} \frac{d\sigma^{ab \rightarrow cd}}{dt} D_{h/c}(z_c, \mu_f). \end{aligned} \quad (17)$$

Here $z_c = p_T/p_{Tc}$, $x_{a,b} = p_{a,b}^+/P_{a,b}^+$. In our notation $\phi_{a,b/N}(x_b, \mu_f)$ are the parton distribution functions (PDFs), $D_{h/c}(z_c, \mu_f)$ are the fragmentation functions (FFs) and we have chosen the factorization/fragmentation, and renormalization scales $\mu_f = \mu_r = p_{Tc}$. The distribution of non-zero transverse momenta of the incoming partons is parametrized as follows

$$f(\mathbf{k}_{a,b}) = \frac{1}{\pi \langle k_{a,b}^2 \rangle} \exp(-\mathbf{k}_{a,b}^2 / \langle k_{a,b}^2 \rangle). \quad (18)$$

The physical requirement for hard partonic scattering is ensured by $k_{a,b} < x_{a,b} \sqrt{s}$ and $K = 1.5$ is a phenomenological K-factor at RHIC. For further details see [6, 8]. Comparison to the PHENIX measurement of π^0 production in $\sqrt{s} = 200$ GeV p+p collisions at RHIC is shown in the insert of Fig. 4.

Nuclear effects can be incorporated in the pQCD formalism, Eq. (17), and fall in two categories: medium-induced kinematic modifications to the perturbative formulas and possibly universal modifications to the PDFs

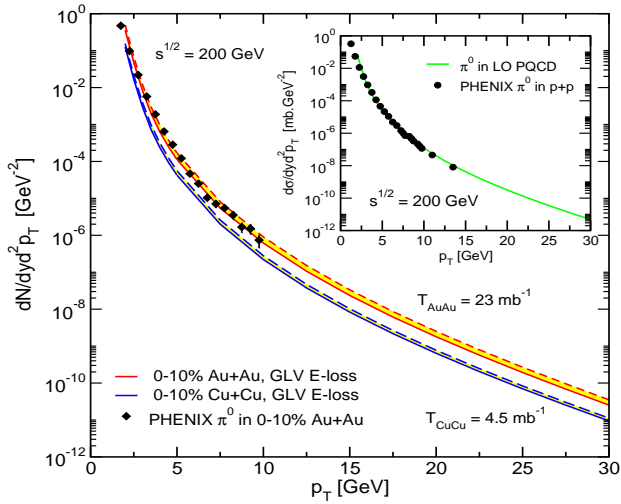


FIG. 4: The predicted invariant multiplicity distribution of neutral pions in central Au+Au collisions at $\sqrt{s} = 200 \text{ GeV}$ for medium density $dN^g/dy = 800 - 1175$ and $T_{AuAu} = 23 \text{ mb}^{-1}$. The same calculation for Cu+Cu collisions for medium density $dN^g/dy = 255 - 370$ and $T_{CuCu} = 4.5 \text{ mb}^{-1}$. The insert shows the cross section for π^0 production in p+p collisions to LO pQCD. Data is from PHENIX [7].

and FFs. An example of the latter are parameterizations of nuclear shadowing $S_{q,g/A}(x, \mu_f)$ [14] included in this calculation via

$$\frac{1}{A} \phi_{q,g/A}(x, \mu_f) = \left(\frac{Z}{A} S_{q,g/A}(x, \mu_f) \phi_{q,g/p}(x, \mu_f) + \frac{N}{A} S_{q,g/A}(x, \mu_f) \phi_{q,g/n}(x, \mu_f) \right). \quad (19)$$

In future work we will combine dynamical calculations of coherent nuclear enhanced power corrections with other elastic and inelastic effects in nuclear matter [14]. Transverse momentum broadening of the incoming partons, leads to enhancement of the differential particle distributions at $p_T \sim \text{few GeV}$ [5] and can be accounted for in Eqs. (17), (18) as follows:

$$\langle k_{a,b}^2 \rangle = \langle k_{a,b}^2 \rangle_{vac} + \langle k_{a,b}^2 \rangle_{med}. \quad (20)$$

Here $\langle k_{a,b}^2 \rangle_{med} = (2\mu^2 L_{a,b}/\lambda_{a,b})\xi$ and the typical momentum transfers squared μ^2 , mean free paths $\lambda_{a,b}$ and parton propagation lengths $L_{a,b}$ refer to cold nuclear matter [5, 6].

In the QGP, final state energy loss is the dominant effect that alters the single and double inclusive hadron production cross sections [5, 6]. Application to the attenuation of leading hadrons as a *kinematic* modification of the momentum fraction z in the FFs $D_{h/c}(z)$ is considered standard [6, 8, 9]. The redistribution of the lost energy in soft and moderate p_T hadrons was only recently derived in the pQCD approach, first for back-to-back two particle correlations [11]. The established dramatic transition from the high p_T factor of four suppression

($R_{AA} \sim 0.25$) to the low p_T factor of two enhancement ($R_{AA} \sim 2$) makes it imperative to study this effect for single inclusive particle production. One possibility is that the fraction of the hadrons from the bremsstrahlung gluons is negligible or small over the full accessible p_T range. At the other extreme, a very large fraction may compromise the current jet quenching phenomenology, leading to $R_{AA} \sim 1$ at moderate transverse momenta even in dense matter.

With this motivation, we first give results for the modification of inclusive hadron production from final state radiative energy loss. It can be represented as:

$$D_{h/c}(z) \Rightarrow \int_0^{1-z} d\epsilon P(\epsilon) \frac{1}{1-\epsilon} D_{h/c}\left(\frac{z}{1-\epsilon}\right) + \int_z^1 d\epsilon \frac{dN^g}{d\epsilon}(\epsilon) \frac{1}{\epsilon} D_{h/g}\left(\frac{z}{\epsilon}\right). \quad (21)$$

Here $P(\epsilon)$ is calculated from Eqs. (10), (15) and $dN_g/d\epsilon$ is the distribution of the average gluons versus $\epsilon = \omega/E$ so that

$$\int_0^1 d\epsilon \frac{dN^g}{d\epsilon}(\epsilon) = \langle N_g \rangle, \quad \int_0^1 d\epsilon \epsilon \frac{dN^g}{d\epsilon}(\epsilon) = \left\langle \frac{\Delta E}{E} \right\rangle. \quad (22)$$

It is easy to verify the momentum sum rule for all hadronic fragments from the attenuated jet and the radiative gluons. With appropriate changes of variables

$$\begin{aligned} \sum_h \int_0^1 dz z D_{h/c}(z) &\Rightarrow \int_0^1 d\epsilon (1-\epsilon) P(\epsilon) \sum_h \int_0^{1-\epsilon} \frac{dz}{1-\epsilon} \frac{z}{1-\epsilon} D_{h/c}\left(\frac{z}{1-\epsilon}\right) \\ &+ \int_0^1 d\epsilon \epsilon \frac{dN^g}{d\epsilon}(\epsilon) \sum_h \int_0^\epsilon \frac{dz}{\epsilon} \frac{z}{\epsilon} D_{h/g}\left(\frac{z}{\epsilon}\right) \\ &= 1 - \langle \epsilon \rangle + \langle \epsilon \rangle = 1. \end{aligned} \quad (23)$$

Figure (4) shows the invariant π^0 multiplicity in central Au+Au and Cu+Cu reactions. Data is from PHENIX [7]. At high p_T , comparisons between the jet quenching theory and the experimental measurement can (and should) also be made for the differential cross sections. At low p_T , a deviation is present due to the fixed order baseline pQCD calculation and QGP effects are more accurately studied via $R_{AA}(p_T)$.

V. QUENCHING OF INCLUSIVE PIONS AT RHIC AND THE LHC

Having evaluated the energy loss of quark and gluon jets in the QGP media specified in Table II, we calculate the quenched pion spectra using Eqs. (17), (19), (20) and (21). Figure 5 shows $R_{AA}(p_T)$ for central, semi-central and peripheral collisions. The predictions

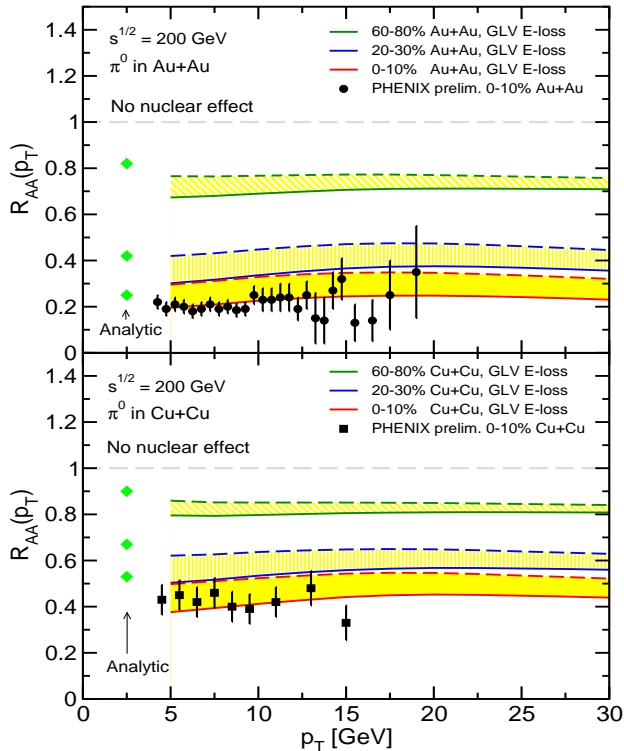


FIG. 5: Top panel: nuclear modification factor R_{AA} for Au+Au collisions at $\sqrt{s} = 200$ GeV versus p_T and centrality. Bottom panel: similar calculation for Cu+Cu at $\sqrt{s} = 200$ GeV at RHIC. Preliminary data is from PHENIX [1] and analytic estimates from Fig. 1 are also shown.

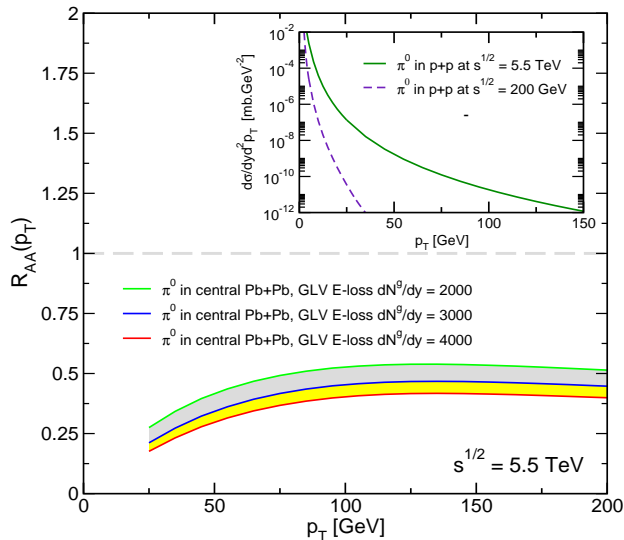


FIG. 6: Suppression of π^0 production in central Au+Au collisions at the LHC as a function of the parton rapidity density. Insert shows the baseline p+p π^0 cross section at $\sqrt{s} = 200$ GeV and $\sqrt{s} = 5.5$ TeV.

in Cu+Cu reactions are for a constant suppression factor, as in Au+Au, at high p_T . Preliminary PHENIX data, first compared to this theory in Ref. [1], are also

included. It should be noted that even in peripheral reactions there can be noticeable particle attenuation. This is larger than the analytic estimates due to sub-leading effects of the medium density on the parton energy loss, discussed in the previous Section, see Fig. 5. Whether such effects are observable or compensated by the non-uniform QGP density in the transverse plane is subject to experimental verification. Finally, we make the important observation that for similar densities and system sizes, for example $dN^g/dy = 410$ in mid-central Au+Au and $dN^g/dy = 370$ in central Cu+Cu, the magnitude of the predicted pion suppression is similar.

Pb+Pb collisions at the LHC represent the future energy frontier of QGP studies in heavy ion reactions. We have explored the sensitivity of $R_{AA}(p_T)$ to the parton rapidity density in central nuclear reactions with $dN^g/dy \simeq 2000, 3000$ and 4000 . In [9] a seven-fold increase of the medium density in going from RHIC to the LHC was assumed. In this work we adhere to a more modest two- to four-fold increase of the soft hadron rapidity density and emphasize that future measurements of jet quenching must be correlated to $dN^g/dy \simeq dN^h/dy \approx (3/2)dN^{ch}/dy$ [6, 8, 12] to verify the consistency of the phenomenological results.

From Figs. 5, 6 and 7 we conclude that at low and moderate p_T , jet suppression at the LHC is larger than at RHIC. However, at high $p_T > 30 - 50$ GeV this ordering is reversed. The physics reason for our result is that the *fractional* energy loss $\langle \Delta E/E \rangle$ of 100 GeV quark and gluon jets at the LHC is not very different from that of 25 GeV jets at RHIC, see Fig. 2. In addition, the power law dependence of the hadronic and the underlying partonic spectrum $n(y, p_{Tc}, \sqrt{s})$ changes (decreases) from $\sqrt{s} = 200$ GeV to $\sqrt{s} = 5.5$ TeV. This is shown in the insert of Fig. 6 and affects the magnitude of calculated nuclear suppression, Eq. (8). LHC will soon provide an extended p_T range to test the correlation of $R_{AA}(p_T)$ with the stiffness of the differential particle spectra.

To assess the importance of the gluon feedback term in Eq. (21), we extend, in Fig. 7, the calculation of $R_{AA}(p_T)$ for central Au+Au and Pb+Pb collisions to low and moderate transverse momenta. At RHIC the redistribution of the lost energy leads to small, $\sim 25\%$, modification of the neutral pion cross section in the $p_T \sim 1 - 2$ GeV range and modest improvement in the theoretical description of that data. In contrast, at the LHC the fragmentation of medium-induced gluons is a much more significant $\geq 100\%$ correction to the low and moderate p_T π^0 production rate.

The need for the more consistent treatment of jet energy loss, Eq. (21), is also illustrated by comparing $R_{AA}(p_T)$ in Fig. 7 to the participant scaling ratio: $(N_{\text{part}}/2)/N_{\text{col}}$ [15]. At high p_T there is no lower limit on the quenching of jets. At low p_T the total available energy of the collision, $\sim (N_{\text{part}}/2)\sqrt{s}$, suggests participant scaling of bulk particle production confirmed by hydrodynamic calculations [16]. Previous estimates of leading particle suppression at low and moderate p_T have vio-

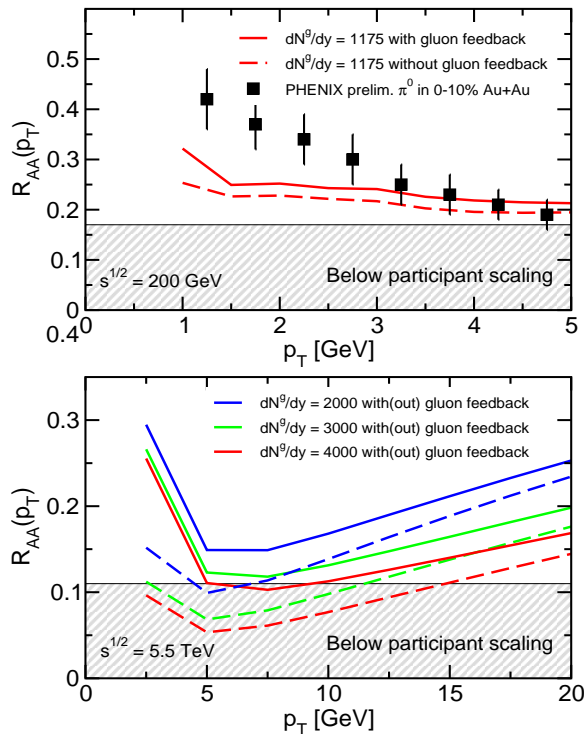


FIG. 7: Top panel: nuclear modification factor R_{AA} in 0-10% central Au+Au collisions at moderate p_T with (solid line) and without (dashed line) gluon feedback, $dN^g/dy = 1175$. Preliminary data is from PHENIX [1]. Bottom panel: nuclear suppression at moderate p_T at the LHC $\sqrt{s} = 5.5$ TeV. Central Pb+Pb collisions with (solid line) and without (dashed line) gluon feedback are shown, $dN^g/dy \simeq 2000, 3000, 4000$.

lated this limit [6, 9]. Fig. 7 shows that the gluon feedback can ensure numerically $R_{AA}(p_T) \geq (N_{\text{part}}/2)/N_{\text{col}}$ at mid-rapidity at the LHC for the densities considered here and is important everywhere in the region $p_T \leq 15$ GeV.

VI. CONCLUSIONS

In this Letter we presented predictions for the nuclear modification of inclusive neutral pion production in Au+Au and Cu+Cu collisions at $\sqrt{s} = 200$ GeV versus

centrality and transverse momentum. Pb+Pb reactions at $\sqrt{s} = 5.5$ TeV at the LHC were also discussed and our calculations at mid-rapidity accounted for Cronin multiple scattering [5], nuclear shadowing [14] and final state radiative energy loss in the quark-gluon plasma [10]. Elastic energy loss was not considered here, since its effects are still under debate [17] relative to the attenuation of jets via gluon bremsstrahlung. We compared our numerical results to a simplified analytic model for centrality dependent jet quenching [6] and showed that there are non-negligible corrections in the evaluation and implementation of radiative energy loss related to the temperature or μ dependence of the strong coupling constant. While the dependence of the observable hadron suppression on dN^g/dy was shown to be sub-linear, this calculation retains sensitivity to both the properties of the medium and the underlying perturbative baseline cross sections.

At low and moderate transverse momenta we derived the contribution to single inclusive pion production from the fragmentation of medium-induced gluons. At RHIC we found this effect to be a modest, $\leq 25\%$, correction. Our result should be contrasted with the case of back-to-back di-hadron correlations where the redistribution of the lost energy controls the QGP-induced transition from suppression to enhancement of large angle inclusive two particle production [11]. At the LHC, however, even in inclusive one pion calculations, gluon feedback is shown to alter the $p_T \leq 15$ GeV cross section in central Pb+Pb reactions by as much as a factor of two. In summary, results reported in this Letter not only provide a more consistent theoretical framework to treat the effects of medium-induced gluon bremsstrahlung but also rectify the over-quenching of jets at low p_T in the limit of large fractional energy loss [6, 9].

Acknowledgments

This research is supported in part by the US Department of Energy under Contract No. W-7405-ENG-3 and by the J. Robert Oppenheimer Fellowship of the Los Alamos National Laboratory.

[1] M. Shimomura [PHENIX Collaboration], nucl-ex/0510023; B. Cole [PHENIX Collaboration], Quark Matter 2005 proceedings.
 [2] J. C. Dunlop [STAR Collaboration], nucl-ex/0510073; P. M. Jacobs and M. van Leeuwen [STAR Collaboration], nucl-ex/0511013.
 [3] M. Gyulassy, nucl-th/0403032; I. Vitev, J. Phys. G **30**, S791 (2004).
 [4] P. Levai *et al.*, Nucl. Phys. A **698**, 631 (2002); K. Adcox *et al.*, Phys. Rev. Lett. **88**, 022301 (2002).

[5] S. S. Adler *et al.* [PHENIX Collaboration], Phys. Rev. Lett. **91**, 072303 (2003); J. Adams *et al.* [STAR Collaboration], Phys. Rev. Lett. **91**, 072304 (2003); I. Vitev, Phys. Lett. B **562**, 36 (2003).
 [6] I. Vitev and M. Gyulassy, Phys. Rev. Lett. **89**, 252301 (2002); X. N. Wang, Phys. Rev. C **70**, 031901 (2004).
 [7] S. S. Adler *et al.*, Phys. Rev. Lett. **91**, 072301 (2003); J. Adams *et al.* [STAR Collaboration], Phys. Rev. Lett. **91**, 172302 (2003).
 [8] A. Adil and M. Gyulassy, Phys. Lett. B **602**, 52 (2004);

- I. Vitev, Phys. Lett. B **606**, 303 (2005).
- [9] S. Turbide, C. Gale, S. Jeon and G. D. Moore, Phys. Rev. C **72**, 014906 (2005); A. Dainese, C. Loizides and G. Paic, Eur. Phys. J. C **38**, 461 (2005).
- [10] M. Gyulassy, P. Levai, I. Vitev, Phys. Rev. Lett. **85**, 5535 (2000); Nucl. Phys. B **594**, 371 (2001).
- [11] I. Vitev, Phys. Lett. B **630**, 78 (2005); J. Adams *et al.* [STAR Collaboration], Phys. Rev. Lett. **95**, 152301 (2005).
- [12] M. Gyulassy, I. Vitev and X. N. Wang, Phys. Rev. Lett. **86**, 2537 (2001).
- [13] F. Arleo, JHEP **0211**, 044 (2002); M. Gyulassy, P. Levai and I. Vitev, Phys. Lett. B **538**, 282 (2002).
- [14] K. J. Eskola, V. J. Kolhinen and C. A. Salgado, Eur. Phys. J. C **9**, 61 (1999); J. W. Qiu and I. Vitev, Phys. Lett. B **632**, 507 (2006).
- [15] With $\sigma_{pp}^{in} = 42$ mb (65 mb) we obtain $(N_{part}/2)/N_{col} = 0.17$ (0.11) at RHIC (LHC), respectively.
- [16] T. Hirano and Y. Nara, Phys. Rev. C **69**, 034908 (2004).
- [17] S. Peigne, P. B. Gossiaux and T. Gousset, JHEP **0604**, 011 (2006); S. Wicks, W. Horowitz, M. Djordjevic and M. Gyulassy, nucl-th/0512076.